J. R. Lyerla
C. S. Yannoni

High-Resolution Carbon-13 NMR of Polymers in the Solid State

This paper reviews the salient features of the methods used for resolution and sensitivity enhancement in ^{13}C NMR spectra of solids. Performance characteristics of the unique variable-temperature cross-polarization magic angle spinning (VT-CPMAS) apparatus developed in our laboratory are given. We present results of structural studies on fluoropolymers using this technique, and discuss the issue of intensities in cross-polarized spectra. In addition, results of an ongoing VT-CPMAS study of polypropylene dynamics are given.

Introduction

Nuclear magnetic resonance is the most powerful analytical tool in organic chemistry, with spectroscopic resolution of one part in 10^9. Because of the large widths of nuclear resonance lines in solids, the atom-by-atom diagnostic capability of NMR has in the past been confined largely to studies of liquid samples. Recent development of techniques for reducing such linewidths by as much as three orders of magnitude [1] has made NMR in solids an attractive method for characterization of bulk solids [2]. The evolution of the spectra shown in Fig. 1, discussed later in detail, underlines the efficacy of the solid state NMR experiment. Indeed, the possibility of being able to study bulk polymers has provided perhaps the greatest single impetus for development of this kind of spectroscopy. Solid state NMR not only provides the opportunity for characterization of polymers as they are used, but also makes possible the study of materials which cannot be dissolved for solution analysis.

This paper reviews the salient features of the methods used for resolution and sensitivity enhancement in ^{13}C NMR spectra of solids. Performance characteristics of the unique variable-temperature cross-polarization magic angle spinning (VT-CPMAS) apparatus developed in our laboratory, which has been described in detail in previous publications, is given [2, 3]. After a brief recounting of selected structural polymer work that we have completed, the results of an ongoing VT-CPMAS study of polypropylene dynamics are presented [2b, 4].

Resolution enhancement in solid state ^{13}C NMR spectra

- *Elimination of dipolar coupling to protons*

The major source of broadening in ^{13}C spectra of organic solids arises from dipolar coupling to protons. This is a through-space coupling, and is the magnetic analogue of coupling between electric dipoles [5]. The coupling between carbon and proton nuclear spins results in splitting in the ^{13}C NMR spectrum. This splitting is given by

$$\Delta\nu = \gamma_H\gamma_C \langle 3\cos^2\theta_{CH} - 1\rangle/4\pi r_{CH}^3, \qquad (1)$$

where γ_H and γ_C are the proton (H) and carbon (C) nuclear gyromagnetic ratios, r_{CH} is the carbon-proton distance, and θ_{CH} is the angle which the C-H vector makes with the external magnetic field B_0. The angular brackets ($\langle \cdots \rangle$) denote an average over the molecular motion. This average is zero for motion in liquids, so that dipolar broadening is absent in solution NMR spectra. In an organic solid, with the rare (1.1% natural abundance) ^{13}C nucleus surrounded by a sea of protons, the carbon resonance is not merely split, but is usually a broad featureless resonance several kilohertz wide. Such a spectrum is shown for a sample of ®Lexan polycarbonate in Fig. 1(a). This width can be reduced significantly by irradiating the protons on resonance, a technique known as *spin decoupling* [6]. The resonant radiation averages the component of the proton magnetic moment along B_0 to zero and eliminates the dipolar coupling and the resultant broadening. Usually, the rf field required for decoupling the protons must be greater than the strength of the dipolar coupling among the protons, which is larger than the $^{13}C-^{1}H$ coupling. The reason for this requirement is that $^{1}H-^{1}H$ dipolar coupling permits rapid mutual spin flips of coupled *proton* magnetic moments. This process, known as *spin diffusion* [5], disrupts the coherent averaging (narrowing) effect of the decoupling rf field. Proton decoupling fields of 1 mT (10 G) are typically required for hydrocarbon polymers. Figure 1(b) shows the improved resolution achieved when proton decoupling is applied while acquiring a solid state ^{13}C spectrum. It is clear that the solid state spectrum is still broad and relatively uninformative, even with decoupling. The residual broadening is due to the ^{13}C chemical shift anisotropy. The next section of this paper is devoted to a discussion of how this broadening can be removed.

• *Elimination of chemical shift anisotropy by magic angle spinning*

The frequency at which a nucleus absorbs radiation in an NMR experiment is called the *chemical shift.* The chemical shift depends on the extent to which the surrounding electrons shield (or deshield) the nucleus from the external magnetic field used in the NMR experiment. Furthermore, the shift δ depends on the orientation of the molecule in the external dc field [7]. This orientational dependence is shown schematically in Fig. 2 for the central (charged) carbon in the t-butyl carbonium ion [8]. In a polycrystalline or amorphous sample, the resonance of a single kind of carbon is a broad asymmetrical pattern which results from the superposition of resonances from molecules in all possible orientations with respect to B_0. For a nucleus in a site of axial symmetry, such as the central carbon in the t-butyl cation, the chemical shift is given by

$$\delta(\phi) = \delta_{\parallel} \cos^2 \phi + \delta_{\perp} \sin^2 \phi, \tag{2}$$

where ϕ is the angle which the *symmetry* axis of the cation makes with B_0. The chemical shift anisotropy (CSA) is defined as the width of such a pattern;

$$\delta(0) - \delta(\pi/2) = \delta_{\parallel} - \delta_{\perp} .$$

As an example, the proton (and fluorine) decoupled spectrum of the central carbon of the t-butyl cation with a fluorinated counter ion (SbF_6^-) is shown in Fig. 3 [8]. The powder pattern for the axially symmetric shift is clearly visible, and the anisotropy (≈450 ppm) is very large. Such a spectrum for a single carbon contains detailed information about the electron density around the nucleus; however, most substances of interest generally have several different kinds of carbons. Overlap of these different powder patterns produces a broad spectrum such as that shown in Fig. 1(b). The effect of magic angle spinning on such spectra is now described.

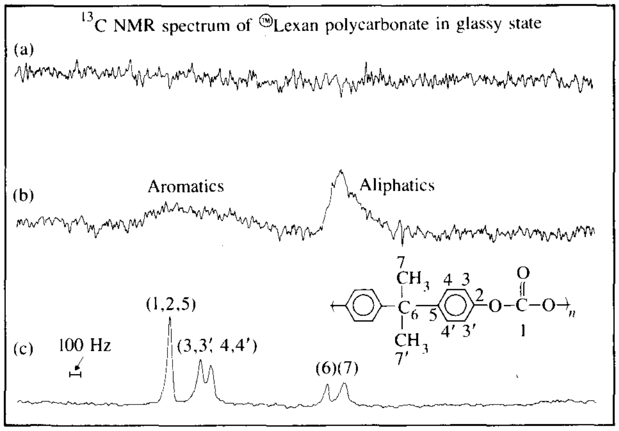

Figure 1 ^{13}C NMR spectra of solid polycarbonate at 27°C. (a) Spectrum obtained under Fourier transform (FT) NMR conditions normal for high resolution on polymer solutions. (b) Spectrum obtained under proton-decoupling cross-polarizing (DD/CP) conditions. (c) Spectrum obtained under DD/CP and magic angle spinning (MAS) conditions. All spectra represent FT of 2000 FID accumulations. Resonance line assignments are given in figure.

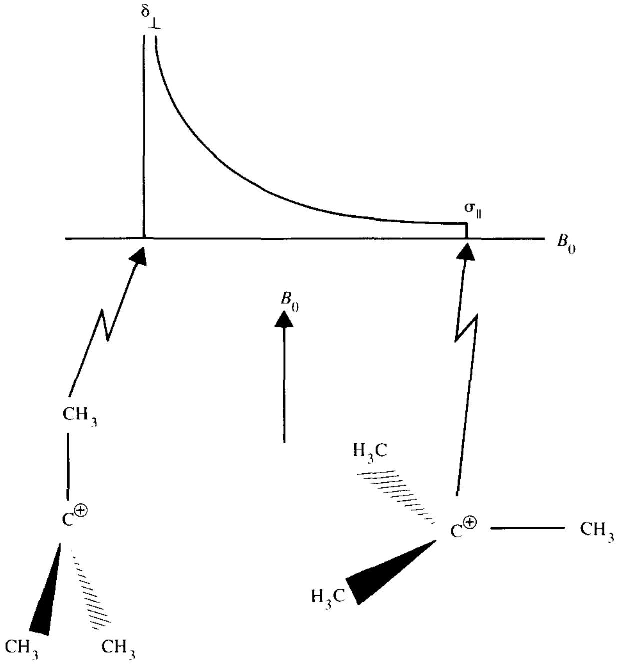

Figure 2 Schematic view of the orientational dependence of chemical shift for the t-butyl carbonium ion.

• *Magic angle spinning*

Perhaps the single most dramatic step in the effort to achieve higher-resolution NMR spectra in solids is the removal of the broad dispersion due to the chemical shift anisotropy. This technique, which requires mechanical rotation of the sample at high speeds [9] (several thousands of revolutions per *second*) results in the transformation of the spectrum of Fig. 1(b) into that shown in Fig. 1(c). This dramatic change is

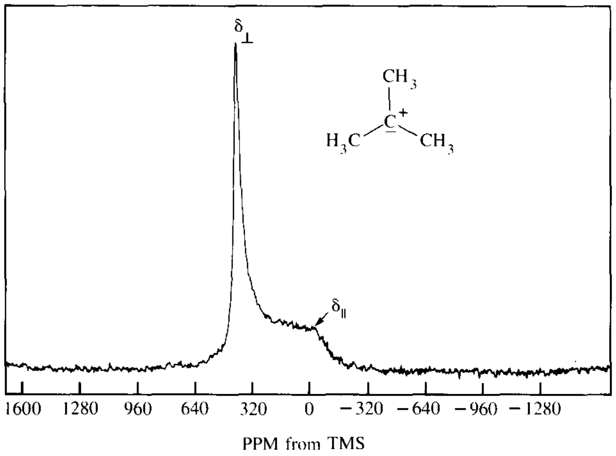

Figure 3 Proton- (and fluorine-) decoupled spectrum of the central carbon in the t-butyl cation with a fluorinated counter ion (SbF_6^-). Overlap of many different powder patterns like these produces a broad spectrum such as that found in Fig. 1(b).

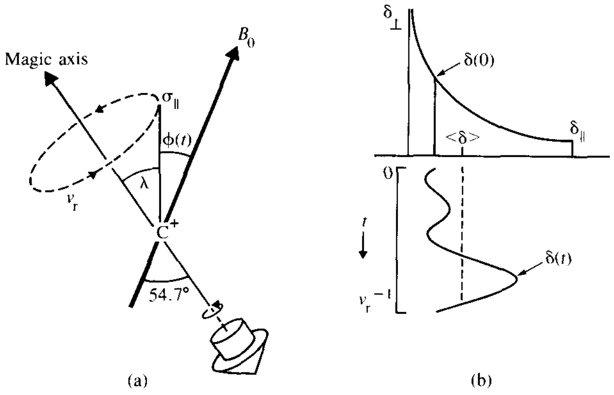

Figure 4 (a) Schematic view of the rotation of the symmetry axis of a single t-butyl cation with an initial orientation $\phi(0)$ about an axis which makes an angle of 54.7° with respect to the external field B_0. (b) Typical time evolution of the chemical shift δ as the sample is rotated. The dashed line indicates the resultant average at the isotropic value.

brought about as follows. The chemical shift [Eq. (2)] can be rewritten as

$$\delta = \langle \delta \rangle + \delta^a, \qquad (3)$$

where $\langle \delta \rangle$ is the isotropic shift observed in solution and δ^a is the anisotropic part of the chemical shift;

$$\delta^a = \frac{1}{3}(\delta_\parallel - \delta_\perp)(3\cos^2\phi - 1). \qquad (4)$$

As shown in Fig. 2, ϕ is the angle which the asymmetry axis in a particular molecule (in this case, a cation) makes with the external field. When the sample is rotated, this angle and the corresponding angular function in Eq. (4) become time-dependent. When the rotation rate is greater than the chemical shift anisotropy (CSA), the anisotropic part of the shift is averaged:

$$\langle \delta^a(t) \rangle = \frac{1}{3}(\delta_\parallel - \delta_\perp)\langle 3\cos^2\phi(t) - 1 \rangle. \qquad (5)$$

The angular brackets imply a time average over a rotational period (ν_r^{-1}) of the sample. Figure 4(a) shows a schematic view of the rotation of the symmetry axis of a single t-butyl cation [with an initial orientation $\phi(0)$] about an axis which makes an angle of 54.7° with respect to the external field (i.e., the "magic" angle). For this geometry, the time average in Eq. (5) can be rewritten as [10]

$$\langle 3\cos^2\phi(t) - 1 \rangle$$

$$= \frac{1}{2}(3\cos^2\gamma - 1)[3\cos^2(54.7°) - 1] = 0, \qquad (6)$$

since $\cos(54.7°) = 1/\sqrt{3}$. It is clear from Eqs. (3)–(5) that, at least for this cation, δ^a is averaged to zero, leaving the average chemical shift at the isotropic value. Figure 4(b) shows a typical time evolution of the chemical shift as the sample is rotated, and the resultant average (dashed line) at the isotropic value. Since the average given in Eq. (6) is zero for the cation regardless of its initial orientation $\phi(0)$, it follows that δ^a becomes zero for all carbons in the sample. Thus, the "magic" of magic angle spinning lies in the fact that spinning around the magic axis reduces *all* CSA powder patterns to the single (isotropic) resonance frequency found in solution. With the narrowing of the CSA patterns, ^{13}C spectra with the resolution shown in Fig. 1(c) are obtained. Although the resolution achieved using these methods is still less than in solution NMR, the atom-by-atom resonance lines make solid state NMR a powerful new analytical technique for studying the properties of bulk polymers on the molecular level.

A brief description is now given of the sensitivity enhancement methods used for solid state NMR spectra.

- *^{13}C signal enhancement in solid state NMR using cross-polarization*

The low natural abundance (1.1%) of the magnetically active ^{13}C isotope makes carbon NMR spectra difficult to detect (in the liquid as well as the solid state). It is possible to enhance ^{13}C spectra of solids by using a technique known as *cross-polarization* (CP) spectroscopy [11]. The method involves a pulse sequence which permits effective cross-relaxation between protons and ^{13}C nuclei. Since cross-relaxation is most effective between nuclei of the same kind, the pulse sequence forces the carbons and protons to process at identical frequencies in their respective rotating frames for a limited duration, called the CP time. Since the precession frequencies are identical, the ^{13}C and ^1H nuclei can undergo energy-conserving spin flips. The ^{13}C-^1H dipolar coupling which is so inimical to good resolution (see previous discussion) is the mechanism by which these "identical" protons and ^{13}C nuclei cross-relax (cross-polarize). After the cross-polarization process is complete, a proton-decoupled time-domain ^{13}C signal is acquired in a conventional manner and stored in a computer. This process is repeated until a sufficient signal-to-noise (S/N) ratio has been obtained. The ^{13}C spectrum is then obtained by a Fourier transformation (FT) of these accumulated time-domain (FID) responses. The CP experiments thus provide ^{13}C signal enhancement in two ways: 1) a gain of carbon magnetization in the cross-polarization process due to the larger proton magnetic moment, and 2) a time saving produced by the ability to repeat the CP sequence after a *proton* polarization time (T_{1H}), rather than having to wait for the longer carbon polarization time (T_{1C}). The sensitivity enhancement gained over a conventional carbon experiment may be given roughly by

$$(S/N)_{CP} = (S/N)_0(\gamma_H/\gamma_C)(T_{1C}/T_{1H})^{1/2}, \qquad (7)$$

where T_{1H} and T_{1C} are the polarization times (also known as the spin-lattice relaxation times) of the protons and carbons in the external dc field. Since $\gamma_H \approx 4\gamma_C$, and since T_{1C} can easily be one or two orders of magnitude longer than T_{1H}, enhancements of four or more can be expected and are often achieved.

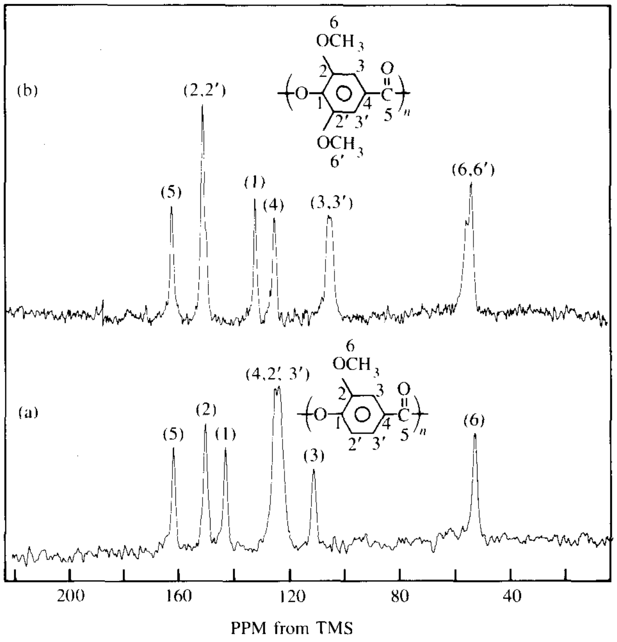

Figure 5 (a) Magic angle CP ^{13}C NMR spectrum of a monomethoxy derivative of p-hydroxybenzoic acid (PHBA) at 27°C. The spectrum was obtained from 2K FT of 21 900 FID accumulations with a CP time of 2.5 ms and experimental repetition times of 3.0 s. (b) Magic angle CP ^{13}C NMR spectrum of dimethoxy derivative of PHBA at 27°C. The spectrum was obtained from 4K FT of 19 000 FID accumulations with other conditions as in (a).

Table 1 Performance characteristics of variable-temperature CPMAS apparatus used in our studies.

Temperature range	15–400 K
Temperature stability	±2 K
Spinning speed at ambient	5 kHz
Spinning speed at 15 K	1.2 kHz
Proton decoupling field at 60 MHz	2.8 mT
Fluorine decoupling field at 56.4 MHz	1 mT

Variable-temperature CPMAS

The unique part of the NMR spectrometer used in the work reported here and elsewhere is a variable-temperature CPMAS apparatus consisting of a spinner and a probe. The apparatus itself has been described in detail in previous publications [2, 3]; Table 1 presents the performance characteristics. The wide temperature range has permitted a variety of studies on systems of interest to organic and polymer chemists [2]. Salient features of some structural studies on polymers using this apparatus are reviewed in the next section.

Polymer structure using CPMAS spectroscopy

- *Aromatic polyesters—linewidths in crystalline and amorphous polymers*

Proton-decoupled ^{13}C CPMAS spectra of the mono- and dimethoxy derivatives of poly(p-hydroxybenzoic acid) (PBHA) are shown in Fig. 5 [12]. The linewidths are $\approx$15 Hz [full width at half maximum (FWHM)]. These lines are, therefore, three to six times narrower than those reported for amorphous materials such as the polycarbonate sample of Fig. 1 ($FWHM$ = 50–100 Hz). The reason for this difference is structural inhomogeneity in the glassy (amorphous) polymers, which leads to distribution of local environments and a concomitant distribution of isotropic chemical shifts [1]. In this picture, a single carbon may experience a slight difference in nuclear shielding (chemical shift) due to a variation in intermolecular effects from one molecule to another in the sample. The shift from one site to the next may be so small that it cannot be resolved as a separate resonance; however, it does result in broadening. These effects have also been observed for the crystalline and noncrystalline regions of a 60% crystalline sample of polyethylene [2b, 13].

- *Intensities in CP spectra*

Our study of polymers has also addressed the issue of intensities in CP spectra. The intensity of a ^{13}C resonance in CP spectroscopy of hydrocarbons is roughly proportional to the square of the strength of the dipolar coupling between the carbon of interest and the proton(s) from which it gains polarization in the CP process. Since dipolar coupling is proportional to the inverse third power of the carbon-proton distance, the CP signal will be weaker for carbons that are not bonded directly to protons. These effects can be exploited to help assign resonances, as shown in Fig. 6 for the parent PBHA [12]. As the CP time is increased, the nonprotonated carbons (C1, C4, and C5) are given more time to gain

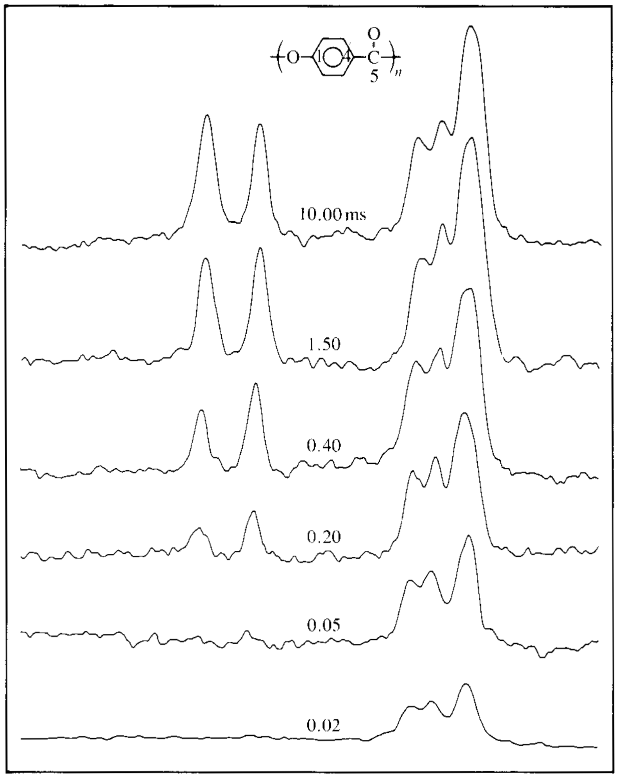

Figure 6 Chemical shifts in poly(p-hydroxybenzoic acid) (PBHA) as a function of the cross-polarization time. The nonprotonated carbons C1, C4, and C5 are absent at short CP times but intensify as the CP time is increased.

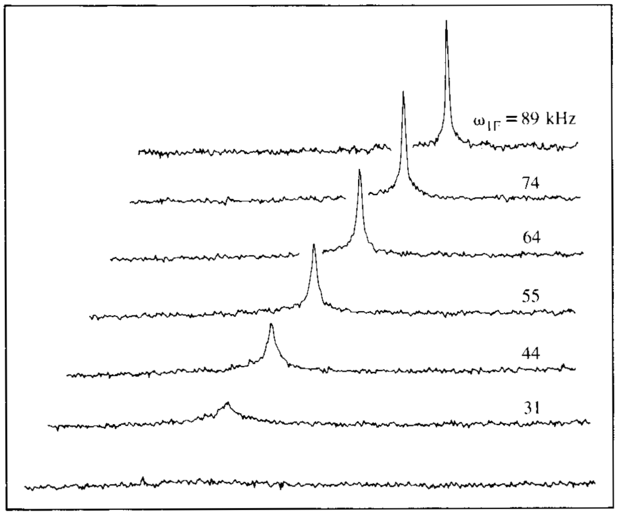

Figure 7 Magic angle spinning (MAS) ^{13}C spectra of poly(tetrafluoroethylene) at -72°C as a function of the ^{19}F decoupling field ω_{1F} in kHz. Each spectrum was obtained from a 2K FT of 256 FID accumulations with a cross-polarization (CP) time of 2 ms. The spectra are displayed on a normalized scale. At ω_{1F} = 89 kHz, the linewidth (FWHM) is approximately 15 Hz.

magnetization from the protons on neighboring carbons. Thus, although the C1, C4, and C5 peaks are absent at short CP times, they intensify as the CP time is increased. This change in intensity clearly helps in the assignment of resonances. By increasing the CP time, it is also possible to obtain spectra which accurately reflect the number of carbons with a given chemical shift [1]. In this respect, CP time variation plays a role similar to the variation in delay between scans in conventionally detected ^{13}C solution spectra.

- *Fluoropolymers*

Some time ago, we extended the CPMAS experiment to obtain ^{13}C spectra of fluoropolymers [14]. The requirement for sufficient ^{19}F decoupling field strengths in fluoropolymers is severe because of the large anisotropy of ^{19}F chemical shifts. This is illustrated in Fig. 7 with a series of spectra of poly(tetrafluoroethylene) as a function of ^{19}F decoupling field strength. The ^{13}C linewidth is still decreasing, even with 2.2 mT (89 kHz) of ^{19}F decoupling. In contrast, linewidths of $\approx$5 Hz (FWHM) can be achieved in semicrystalline polyethylene with only 35–40 kHz of ^{1}H decoupling, since the CSA of protons is an order of magnitude smaller than for ^{19}F in the corresponding fluorocarbon.

The discussion of the effect of broadening by quadrupolar nuclei applies to all solid state NMR spectra [15], but is illustrated in Fig. 8 with temperature-dependent ^{13}C spectra of a halogenated fluoropolymer, poly(chlorotrifluoroethylene) (PCTFE) [14]. At ambient and higher temperatures, the peaks from the CF_2 and CFCl carbons are of equal height and intensity, as expected. As the temperature is lowered, however, the line due to the chlorine-bearing carbon broadens and becomes very weak at -70°C. We attribute this behavior to broadening by the ^{35}Cl nucleus, which has a spin quantum number of 3/2 and a large electric quadrupole moment. The quadrupole moment couples, via the electric quadrupole interaction, to the gradient of the electric field caused by electrons surrounding the nucleus. If the quadrupole interaction is larger than the forces which align the ^{35}Cl magnetic moment along the external magnetic field used in the NMR experiment, all the line-narrowing methods discussed so far will have little effect on the behavior of the ^{35}Cl magnetic moment. Thus, the ^{13}C may experience broadening due to dipolar coupling with the ^{35}Cl moment, and this broadening may be impossible to remove by known methods. For covalent C-Cl bonding, such as in PCTFE, the quadrupole interaction is indeed large, and we believe that the reduction of height of the chlorinated carbon peak is due to an increase in the strength of dipolar coupling to the ^{35}Cl moment as the temperature is lowered.

At high temperature, it is likely that molecular motion relaxes the ^{35}Cl magnetic moment via quadrupole relaxation rapidly enough to "self-decouple" it from the ^{13}C nuclear moment to which the chlorine is bonded [16]. We have also observed similar temperature-dependent broadening in ^{13}C spectra of carbocations associated with a chlorinated counter ion [2b]. The broadening effects of quadrupolar nuclei such as ^{14}N are also well documented [14, 17], and generally degrade resolution in solid state NMR spectra.

The results summarized in this section constitute but a small part of a growing literature on structural studies of polymers, and serve to highlight a number of characteristics peculiar to solid state NMR spectroscopy. In the next section we present recent results of an ongoing study of molecular dynamics in polypropylene.

Relaxation measurements of polypropylene in the solid state

One of the principal advantages of CPMAS experiments is that resolution in the solid state allows individual-carbon relaxation experiments to be performed. If a sufficient number of unique resonances exist, the results can be interpreted in terms of rigid-body and local motions (e.g., methyl rotation, segmental modes in polymers, etc.) [18, 19]. This presents a distinct advantage over the more common proton relaxation measurements, in which efficient spin diffusion usually results in averaging of relaxational behavior over the ensemble of protons to yield a single relaxation time for all protons. This makes interpretation of the data in terms of unique motions difficult.

Relaxation parameters of interest for the study of organic solids and polymers include 1) ^{13}C and ^{1}H spin-lattice relaxation times (T_{1C} and T_{1H}), 2) the spin-spin relaxation time T_2, 3) the nuclear Overhauser enhancement (NOE), 4) the proton and carbon rotating-frame relaxation times ($T^{C}_{1\rho}$ and $T^{H}_{1\rho}$), 5) the C-H cross-relaxation time T_{CH}, and 6) the proton relaxation time in the dipolar state, T_{1D} [19]. Not all of these parameters provide information in a direct manner; nonetheless, the inferred information is important in characterizing motional frequencies and amplitudes in solids. The measurement of data over a range of temperatures is fundamental to this characterization.

Before discussing relaxation measurements, it is worthwhile to note the importance of VT-MAS from the purely operational point of view. Often the presence of unfavorable relaxation times ($T_{1\rho}$, T_1) makes cross-polarization inefficient at a given temperature. For example, polyethylene oxide (PEO) has a minimum in its proton $T_{1\rho}$ value at ambient temperature [20]. This results in a very weak ^{13}C signal via cross-polarization since the proton order is destroyed before polarization transfer has proceeded to a significant degree. However, at temperatures below −60°C, $T^{H}_{1\rho}$ is sufficiently long that CP techniques may be used to obtain efficiently ^{13}C spectra of PEO in the bulk [21].

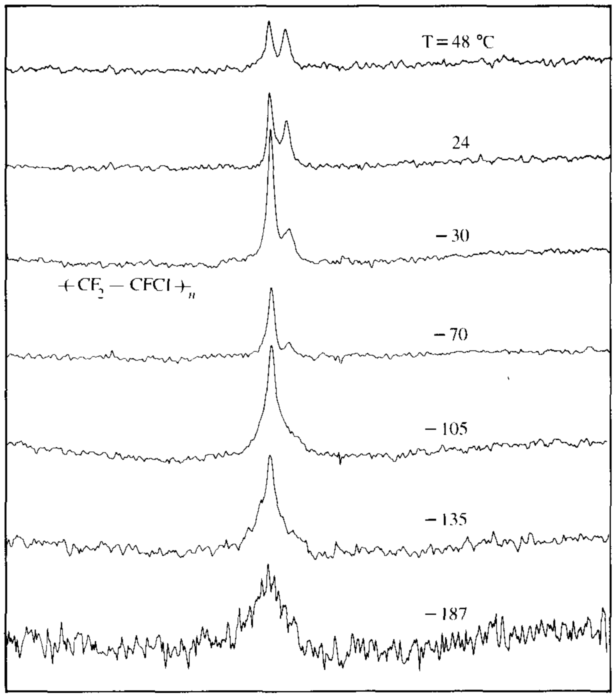

Figure 8 Fluorine-decoupled CPMAS ^{13}C spectra of poly(chlorotrifluoroethylene) (PCTFE) as a function of temperature.

The measurements of carbon T_1 and $T_{1\rho}$ provide information on molecular motions in the MHz and kHz frequency ranges, respectively. Again, Schaefer and Stejskal have carried out pioneering ^{13}C work in their investigations of glassy polymers [18, 19]. In particular, they stress the utility of $T_{1\rho}$ measurements for probing the dynamic heterogeneity of the glassy state, and as a potential source of insight into the mechanical properties of polymers at the molecular level. Garroway and coworkers [22] reported the first VT-MAS $T_{1\rho}$ results in their study of epoxy resins, and together with VanderHart [23] have emphasized the complications involved in interpreting $T_{1\rho}$ in terms of lattice (motional) processes.

Recently, we have obtained the first extensive subambient VT-MAS ^{13}C T_1 and $T_{1\rho}$ data on macromolecules. The emphasis of the study was placed on isotactic polypropylene (PP) and atactic poly(methyl methacrylate) (PMMA), since they represent semicrystalline and glassy polymers, respectively. Specifics of the investigation were directed to the issue of elucidating sidechain and backbone motions from the high-frequency relaxation experiments. Samples were machined into the shape of Andrew-type rotors, and used directly in the studies. Spin relaxation times T_1 were collected using a pulse sequence developed by Torchia [24], which allows cross-polarization enhancement of the signals. The $T_{1\rho}$ data were determined at 57 kHz by using the $T_{1\rho}$ methodology of Schaefer et al. [18]. The PP examined was a 90% isotactic, 70% crystalline sample. The PMMA was an atactic commercial polymer.

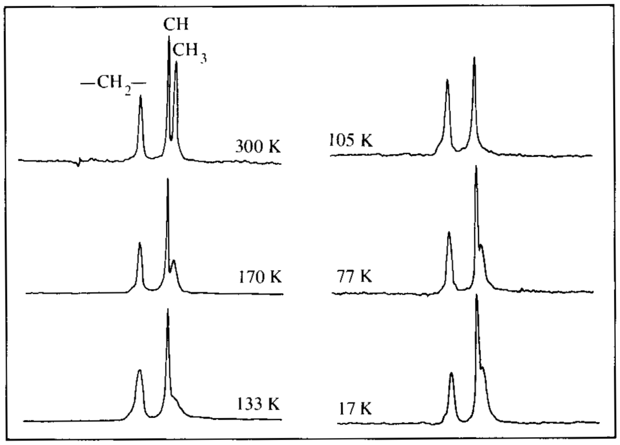

Figure 9 CPMAS ^{13}C spectra of polypropylene as a function of temperature.

Figure 9 shows the CPMAS ^{13}C spectra of PP as a function of temperature. The interesting feature is the progressive broadening of the methyl resonance as the temperature is lowered. At $\approx$110 K, the resonance is broadened to the point of disappearing from the spectrum. However, at temperatures below 77 K, the methyl resonance narrows and reappears in the spectrum. This broadening phenomenon arises as the reorientation rate of the methyl group about the C_3 axis becomes insufficient to average (stochastically) dipolar interaction with the methyl protons. At the onset of broadening, the methyl motion has a correlation time comparable to the inverse of the strength (in frequency units) of the proton decoupling field. This reduces the efficiency of the rf decoupling and leads to a maximum linewidth of the carbon when the motions occur at the frequency corresponding to the amplitude of the proton decoupling field.

Rothwell and Waugh [25] have developed the theory for T_2 (the inverse of the ^{13}C linewidth) for an interplay between stochastic and coherent motions. For such a system, the profile of linewidth vs. temperature shows a maximum when the correlation time for molecular motion, τ_c, is equal to the modulation period of the decoupling, $(1/\omega_1)$. In the "short correlation" limit ($\omega_1\tau_c << 1$) (high temperature), the linewidth is reduced by the rapid motional averaging, while in the "long correlation" limit ($\omega_1\tau_c >> 1$) (low temperature), the linewidth is reduced by efficient decoupling of C-H dipolar interactions. The spectra of PP in Fig. 9 are consistent with the progression of the methyl resonance through the linewidth regions as the temperature is lowered. The reappearance (narrowing) of the methyl resonance at 77 K indicates that the "long correlation time" regime has been reached [26]. Further proof of the progressive changes in correlation time for methyl rotation as the temperature is lowered is provided by the field dependence of the linewidth shown in the figure. At about 160 K, the methyl linewidth is independent of decoupling field, while at 77 K the linewidth varies as the inverse square of the decoupling field. This is the expected dependence for the transition between the extreme narrowing and long correlation time regimes [25]. Finally, from the expression for the ^{13}C linewidth derived by Rothwell and Waugh [Eq. (8)] and the correlation time and temperature of the $T_{1\rho}^{H}$ minimum observed by McBrierty et al. [26],

$$\frac{1}{T_2} = \frac{\gamma_C^2\gamma_H^2\hbar^2}{5r_{CH}^6}\left(\frac{\tau_c}{1+\omega_1^2\tau_c^2}\right), \tag{8}$$

we calculate, for $\omega_1 = 57$ kHz (the value of the decoupling field used to obtain the spectra in Fig. 9), that the maximum broadening for the methyl resonance would occur at 109 K, in excellent agreement with our observations.

This broadening of the methyl resonance observed in PP is also found in polycarbonate, PMMA, and epoxy polymers. It should be a general phenomenon for rapidly reorienting side groups or main-chain carbons in polymers. For semicrystalline systems, where the local molecular structure is relatively homogeneous, severe broadening should result in the "disappearance" of resonance lines from the spectra. For glassy systems, where there is more heterogeneity in the local molecular environment, the effect may result in significant changes in resonance lineshape as a function of temperature as the carbons in differing environments undergo severe broadening. Of course, the phenomenon may be used to determine τ_c for the group undergoing the motion [25]; however, the severe broadening does limit the ability to measure high-frequency relaxation times in such temperature intervals.

The ^{13}C spin-lattice relaxation times for isotactic PP are shown in Fig. 10. Over the temperature range, each carbon in the repeat unit displays an individual relaxation time. Primarily, the data represent that of the crystalline component. The semilog plots of intensity vs. time were nearly exponential for each of the carbons at all temperatures. The backbone carbon T_1 values are one to two orders of magnitude longer than the methyl carbon. If it is assumed that a C-H heteronuclear relaxation mechanism is operative, this suggests that backbone motion is either very slow or of a very small amplitude. The methyl relaxation appears to be dominated by methyl C_3 reorientation. A calculation of the methyl carbon relaxation time based on a Bloembergen-Purcell-Pound (BPP) formalism and the correlation time at the proton T_1 minimum [26] at -110°C gives a value of 10 ms at -110°C, in good agreement with the observed value of 17 ms. In addition, the methyl motion also seems to dominate the backbone relaxation. This is evidenced by the shorter T_1 observed for the methine carbon relative to methylene (despite there being two direct C-H interactions for the methylene carbon). Apparently, backbone motions are character-

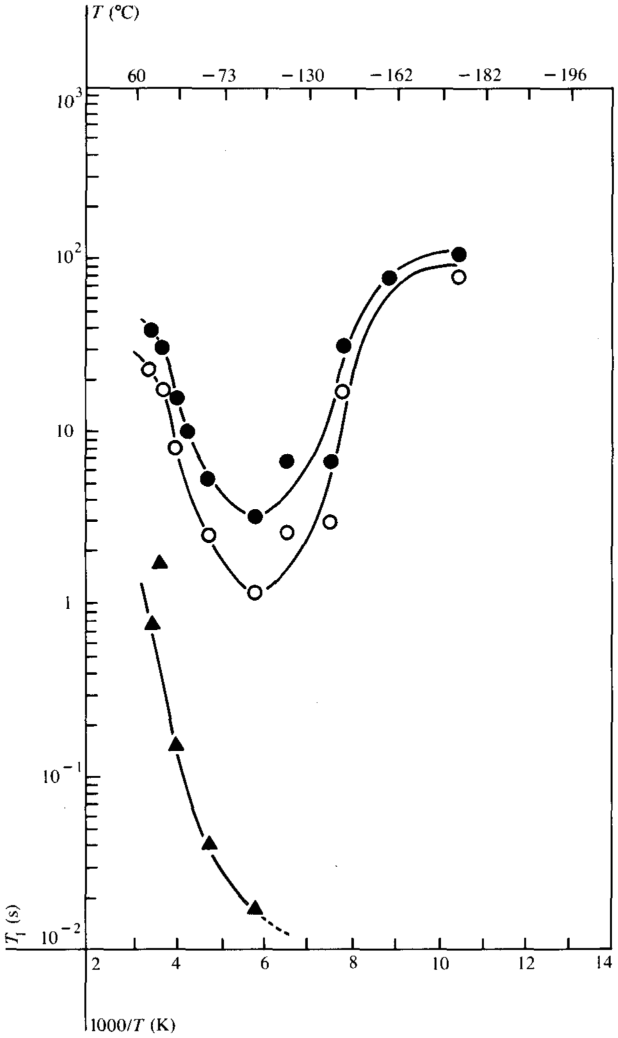

Figure 10 The ^{13}C spin-lattice relaxation times for isotactic polypropylene methylene (●), methine (○), and methyl (▲) carbons.

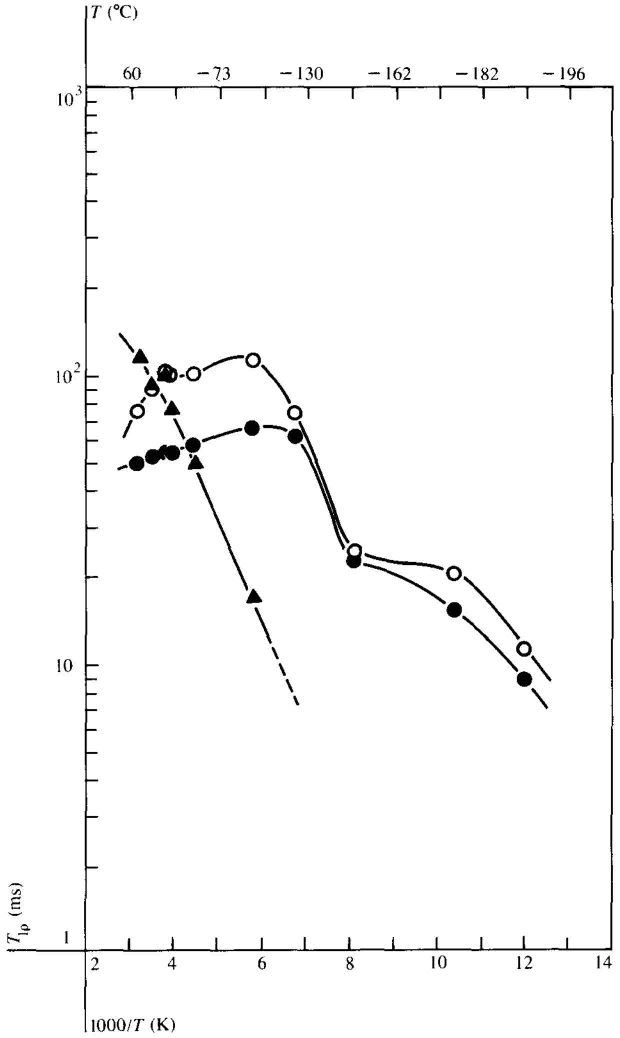

Figure 11 The $T_{1\rho}$ data for CH (○), CH_2 (●), and CH_3 (▲) carbons in polypropylene.

ized by such small amplitudes and low frequencies that contributions from the direct C-H interactions to spectral density in the MHz region of the frequency spectrum are minor relative to those from side groups. The $1/r^6$ distance dependence of dipolar relaxation thus accounts for both the long T_1 values of CH and CH_2 carbons relative to the methyl carbon and the shorter T_1 values for methine carbons relative to methylene carbons. The fact that the observed T_1 minimum for CH and CH_2 carbons is close to that reported for a proton T_1 minimum (at 30 MHz) [26] in PP that was assigned to methyl reorientation provides unequivocal support for the dominance of the T_1 relaxation by methyl protons.

The $T_{1\rho}$ data (Fig. 11) for the CH and CH_2 carbons also give an indication of methyl group rotational frequencies. As the temperature is lowered below 163 K, the T_1 for these carbons increases and the $T_{1\rho}$ decreases by roughly an order of magnitude between 163 K and 95 K, suggesting that the contribution of methyl proton motion to MHz spectral density is decreasing, while increasing in the kHz regime. The CH and CH_2 $T_{1\rho}$ do not change greatly over the temperature interval from 163 K to ambient, and, in contrast to the T_1 behavior, the CH_2 carbon has the shorter $T_{1\rho}$. The interpretation of the carbon $T_{1\rho}$ data is complicated by the fact that spin-spin (cross-relaxation) processes, as well as rotating-frame spin-lattice processes, contribute to the relaxation [23, 27]. Only the latter provide direct information on molecular motion. Although both processes show a dependence on the number of nearest-neighbor protons, the relative insensitivity of $T_{1\rho}$ to temperature and the approximate 2:1 ratio of CH_2/CH T_{CH} values also suggest that spin-spin processes dominate the relaxation above 163 K [27]. Below 163 K, the $T_{1\rho}$ of both carbons shorten and tend toward equality, indicating that spin-lattice processes derived from

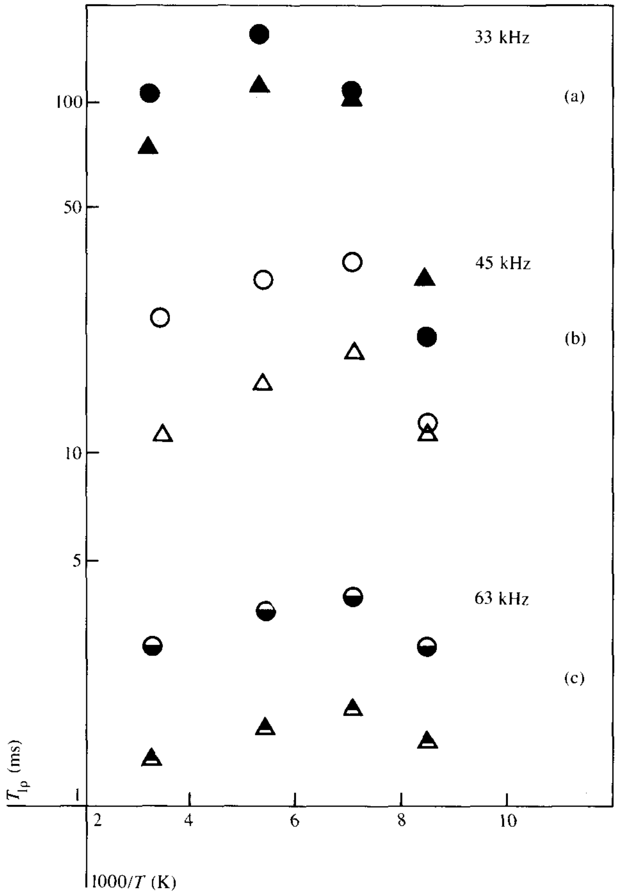

Figure 12 The $T_{1\rho}$ for methine (circles) and methylene (triangles) carbons in polypropylene as a function of the rotating-frame field and the temperature; (a) 33 kHz, (b) 45 kHz, and (c) 63 kHz.

Table 2 ^{13}C $T_{1\rho}$ formalism.

Motion: BPP dipolar

$$\frac{1}{T_{1\rho}^{C}} = \frac{N_H \gamma_H^2 \gamma_C^2}{20 r_{CH}^6} f(\tau_c)$$

$$f(\tau_c) = \left\{ 2J(\omega_1) + \frac{J(\omega_H - \omega_C)}{2} + \frac{3J(\omega_C)}{2} + 3J(\omega_H) + 3J(\omega_H + \omega_C) \right\}$$

$$J(\omega_i) = 2\tau_c/(1 + \omega_i^2 \tau_c^2)$$

For long τ_c, $\frac{1}{T_{1\rho}^{C}} \propto \frac{1}{\omega_i^2}$

Spin effects:

$$\frac{1}{T_{1\rho}^{C}} = \frac{1}{2} \sin^2 \theta_s M_{CH}^{(2)} J_D(\omega_{1C})$$

$$J_D(\omega) = \pi \tau_D \, e^{-|\omega_{1C}| \tau_D}$$

$$\frac{1}{T_{1\rho}^{C}} \propto e^{2\pi \nu_{1C} \tau_D}$$

methyl reorientation are becoming competitive with the spin-spin process in relaxing the backbone carbon magnetization. McBrierty et al. [26] report a proton $T_{1\rho}$ minimum at 97 K, which reflects methyl reorientation at kHz frequencies. No clear minimum is observed in the ^{13}C data, perhaps due to the interplay of the spin-spin and spin-lattice processes. Nonetheless, it is apparent that the methyl protons are responsible for the spin-lattice contributions to the CH and CH_2 $T_{1\rho}$ values.

Further evidence for the effect of spin-spin processes on $T_{1\rho}$ in PP is given in Fig. 12, which shows $T_{1\rho}$ as a function of the rotating-frame field plotted against the reciprocal of the temperature. As indicated in Table 2, in the case of a motion-dominating $T_{1\rho}$, there is a square dependence of T_1 on field. For spin-spin domination, there is an exponential dependence. The results at room temperature clearly display a dependence greater than the 4× suggested for motion and the field variation. Only at temperatures less than 150 K with large rotating-frame fields are strong motional effects observed. As previously discussed, these arise from methyl rotation.

The domination of both spin-lattice relaxation times for CH and CH_2 carbons in PP by methyl reorientation is clearly disappointing, since the potential for information on backbone motion due to the high resolution of the CPMAS experiments is not realized. The implication is that it may not be possible to observe backbone motion in crystalline materials having rapidly reorienting side groups without resorting to deuterium substitution of these side groups.

The T_1 data for various carbons in PMMA are given in Fig. 13. Clear deviations from nonexponential behavior were often observed. Behavior different from that observed for PP presumably arises because the high degree of stereoregularity and high crystallinity of the PP provide a more homogeneous local environment than in glassy PMMA, where

Table 3 ^{13}C $T_{1\rho}$ data for poly(methyl methacrylate) (PMMA).

Temperature (K)	*Carbon T_1 (ms)*			
	$-CH_3$	*$-C{=}O$*	*$-C-$*	*$-OCH_3$*
293	26	271	187	135
253	14	343	174	227
213	5	134	118	164
193	—	139	98	156
173	—	102	104	124
133	11	294	158	157
113	31	366	186	132
78	23	314	178	82

distributions of relaxation times are commonly observed, owing to site heterogeneity. For PMMA, the reported relaxation times represent the long-time portion of the magnetization decay curves.

The results for PMMA tend to cluster over the temperature range studied, except for the α-methyl carbon. The rapid relaxation for carbon in the temperature range from 20°C to -70°C is consistent with the proton T_1 minimum at about -23°C assigned to α-methyl rotation at MHz frequencies [28].

The $T_{1\rho}$ data for PMMA are summarized in Table 3. As in the case of PP, the α-CH_3 undergoes motional broadening and disappears from the spectrum near the minimum in $T_{1\rho}$. In PMMA, severe broadening occurs in the temperature range between 140 K and 200 K. At lower temperatures, the α-methyl carbon line narrows as the decoupling becomes effective. The $T_{1\rho}$ data for the quaternary carbonyl and methoxy carbons also reflect the methyl motion. Again, this demonstrates the effectiveness of methyl motion in relaxing other carbons in solids via long-range C-H dipolar interactions. Thus, despite the resolution of the CPMAS experiment, the extraction of information on local motional rates from carbon T_1 and $T_{1\rho}$ data on PMMA is not as straightforward as anticipated.

Acknowledgment

The authors wish to acknowledge the skillful and innovative technical assistance of R. D. Kendrick.

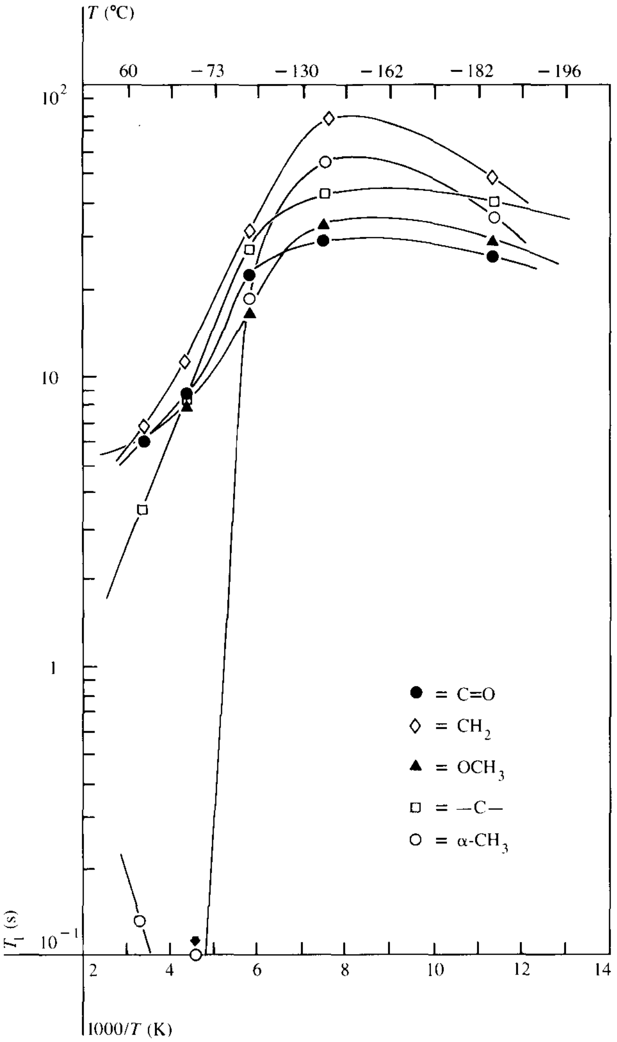

Figure 13 The $T_{1\rho}$ data for various carbons in poly(methyl methacrylate).

References and note

1. J. Schaefer, E. O. Stejskal, and R. Buchdahl, "Magic-Angle ^{13}C NMR Analysis of Motion in Solid Glassy Polymers," *Macromol.* **10,** 384–405 (1977).
2. (a) C. S. Yannoni, "High-Resolution NMR in Solids: The CPMAS Experiment," *Accts. Chem. Res.* **15,** 201–208 (1982); (b) J. R. Lyerla, C. S. Yannoni, and C. A. Fyfe, "Chemical Applications of Variable-Temperature CPMAS NMR Spectroscopy in Solids," *Accts. Chem. Res.* **15,** 208–216 (1982).
3. C. A. Fyfe, H. Mossbruger, and C. S. Yannoni, "A Simple 'Magic-Angle' Spinning Apparatus for Routine Use in NMR Spectroscopy of Solids," *J. Magn. Reson.* **36,** 61–68 (1979).
4. W. W. Fleming, C. A. Fyfe, R. D. Kendrick, J. R. Lyerla, H. Vanni, and C. S. Yannoni, "Variable-Temperature Magic-Angle Spinning Carbon-13 NMR Studies of Solid Polymers," *ACS Symposium Series* **142,** 193–217 (1980).
5. A. Abragam, *The Principles of Nuclear Magnetism,* Oxford University Press, London, 1961, Ch. IV.
6. *Ibid.,* p. 571.
7. U. Haeberlen, "High Resolution NMR in Solids, Selective Averaging," *Advances in Magnetic Resonance,* Supplement 1, J. S. Waugh, Ed., Academic Press, Inc., New York, 1976, Ch. 3.
8. P. C. Myhre and C. S. Yannoni, "^{13}C NMR Spectra of Carbonium Ions in the Solid State: The sec-Butyl Cation," *J. Amer. Chem. Soc.* **103,** 230–232 (1981).
9. I. J. Lowe, "Free Induction Decays of Rotating Solids," *Phys. Rev. Lett.* **2,** 285–287 (1959); E. R. Andrew, *Arch. Sci.* (Geneva) **12,** 103 (1959); E. R. Andrew, "The Narrowing of NMR Spectra of Solids by High-Speed Specimen Rotation and

the Resolution of Chemical Shift and Spin Multiplet Structures for Solids," *Progress in Nuclear Magnetic Resonance Spectroscopy*, Vol. 8, J. W. Emsley, J. Feeney, and L. H. Sutcliffe, Eds., Pergamon Press, Inc., New York, 1971, pp. 1–39.

10. H. Margenau and G. M. Murphy, *The Mathematics of Physics and Chemistry*, Van Nostrand, New York, 1956, pp. 109–113.
11. A. Pines, M. G. Gibby, and J. S. Waugh, "Proton-Enhanced NMR of Dilute Spins in Solids," *J. Chem. Phys.* **59**, 569–590 (1973).
12. C. A. Fyfe, J. R. Lyerla, W. Volksen, and C. S. Yannoni, "High-Resolution Carbon-13 Nuclear Magnetic Resonance Studies of Polymers in the Solid State. Aromatic Polyesters," *Macromol.* **12,** 757–761 (1979).
13. W. L. Earl and D. L. VanderHart, "Observations in Solid Polyethylenes by Carbon-13 Nuclear Magnetic Resonance with Magic Angle Sample Spinning," *Macromol.* **12,** 762–767 (1979).
14. W. W. Fleming, C. A. Fyfe, J. R. Lyerla, H. Vanni, and C. S. Yannoni, "Variable Temperature High-Resolution Carbon-13 NMR Spectra of Solid Fluoropolymers," *Macromol.* **13,** 460–462 (1980).
15. E. Lippmaa, M. Alla, and E. Kundla, "Line Splittings Through Dipole-Dipole Interaction with Quadrupole Nuclei in ^{13}C High Resolution NMR Powder Spectra," presented at the 18th Experimental NMR Conference, Asilomar, CA, April 1977; E. M. Menger and W. S. Veeman, "Quadrupole Effects in High-Resolution Phosphorus-31 Solid-State NMR Spectra of Triphenyl Phosphene Copper (I) Complexes," *J. Magn. Reson.* **46,** 257–268 (1982).
16. H. W. Spiess, U. Haeberlen, and H. Zimmermann, "^{1}H Multiple-Pulse Study of a Single Crystal of trans-Diiodoethylene: Example of Self-Decoupling," *J. Magn. Reson.* **25,** 55–66 (1977).
17. E. Lippmaa, M. Alla, T. J. Pehk, and G. Engelhardt, "Solid-State High Resolution NMR Spectroscopy of Spin 1/2 Nuclei (^{13}C, ^{29}Si, ^{119}Sn) in Organic Compounds," *J. Amer. Chem. Soc.* **100,** 1929–1931 (1978).
18. J. Schaefer, E. O. Stejskal, and R. Buchdahl, "High-Resolution Carbon-13 Nuclear Magnetic Resonance Study of Some Solid, Glassy Polymers," *Macromol.* **8,** 291–296 (1975); "Magic-Angle ^{13}C NMR Analysis of Motion in Solid Glassy Polymers," *Macromol.* **10,** 384–405 (1977).
19. J. R. Lyerla, in *Contemporary Topics in Polymer Science*, Vol. 4, M. Shen, Ed., Plenum Publishing Co., New York, 1979, pp. 143–213 and references therein. J. Schaefer, M. D. Sefcik, E. O. Stejskal, and R. A. McKay, "Magic-Angle Carbon-13 Nuclear Magnetic Resonance Analysis of the Interface between Phases in a Blend of Polystyrene with a Polystyrene-Polybutadiene Block Copolymer," *Macromol.* **14,** 188–192 (1981) and references therein. S. J. Opella, M. H. Frey, and T. A. Cross, "Detection of Individual Carbon Resonances in Solid Proteins," *J. Amer. Chem. Soc.* **101,** 5856–5857 (1979). W. L. Earl and D. L. VanderHart, "High Resolution, Magic Angle Sample Spinning ^{13}C NMR of Solid Cellulose I," *J. Amer. Chem. Soc.* **102,** 3251–3252 (1980). R. H. Atalla, J. G. Gast, D. W. Sindorf, V. J. Bartuska, and G. E. Maciel, "^{13}C NMR Spectra of Cellulose Polymorphs," *J. Amer. Chem. Soc.* **102,** 3249–3251 (1980).
20. T. M. Conner, in *NMR Basic Principles and Progess*, Vol. 4, Springer-Verlag, New York, 1971, pp. 247–270.
21. W. W. Fleming, C. A. Fyfe, R. D. Kendrick, J. R. Lyerla, H. Vanni, and C. S. Yannoni, "Polymer Characterization by ESR and NMR," *ACS Symposium Series* **142,** 193–218 (1980).
22. A. N. Garroway, W. B. Moniz, and H. A. Resing, "^{13}C NMR in Cured Epoxies: Benefits of Magic Angle Rotation," *Div. Org. Coatings Plastics Preprints* **36,** 133–138 (1976). A. N. Garroway, W. B. Moniz, and H. A. Resing, "Carbon-13 NMR in Organic Solids: The Potential for Polymer Characterization," *ACS Symposium Series* **103,** 67–87 (1979).
23. D. L. VanderHart and A. N. Garroway, "^{13}C NMR Rotating Frame Relaxation in a Solid with Strongly Coupled Protons: Polyethylene," *J. Chem. Phys.* **71,** 2773–2787 (1979).
24. D. A. Torchia, "The Measurement of Proton-Enhanced Carbon-13 T_1 Values by a Method Which Suppresses Artifacts," *J. Magn. Reson.* **30,** 613–616 (1978).
25. W. P. Rothwell and J. S. Waugh, "Transverse Relaxation of Dipolar Coupled Spin Systems under RF Irradiation: Detecting Motions in Solids," *J. Chem. Phys.* **74,** 2721–2732 (1981).
26. V. J. McBrierty, D. C. Douglass, and D. R. Falcone, "Nuclear Magnetic Relaxation in Polypropylene," *J. Chem. Soc. Faraday Trans. II* **68,** 1051–1059 (1972).
27. If spin-spin effects dominate the rotating-frame relaxation and the carbon cross-relaxation to the proton dipolar reservoir is less efficient than the corresponding proton spin-lattice relaxation T_{1D}, the observed $T_{1\rho}$ for the CH carbon will be about 1.7–2.0× that of the CH_2 carbon, based on the approximate twofold difference in the second moments (due to protons) for the two types of carbons. This is roughly the result observed in the data displayed in Fig. 11.
28. J. G. Powles and P. Mansfield, "Molecular Motion in Polymethylmethacrylate by Proton Spin-Lattice Relaxation," *Polymer* **3,** 336–339 (1962).

Received March 25, 1983

James R. Lyerla *IBM Research Division, 5600 Cottle Road, San Jose, California 95193.* Dr. Lyerla is manager of the polymers for storage applications group in the polymer science and technology department at San Jose. He is currently involved in basic research in the application of nuclear magnetic and resonance spectroscopy to the study of polymer structure and polymer chain dynamics in the bulk state. Dr. Lyerla joined IBM at the San Jose laboratory in 1975 after completing a National Research Council/National Academy of Sciences Research Associateship at the National Bureau of Standards. He received a B.A. in chemistry in 1966 from Southern Illinois University, Carbondale, and a Ph.D. in physical chemistry in 1971 from the University of Utah. Dr. Lyerla is a member of the American Chemical Society and the American Physical Society.

Costantino S. Yannoni *IBM Research Division, 5600 Cottle Road, San Jose, California 95193.* Dr. Yannoni is a research staff member in the Chemical Dynamics Department at San Jose, involved in determination of structure and dynamics using solid-state nuclear magnetic resonance techniques. In 1967, he joined IBM at the Thomas J. Watson Research Center, where he worked on general chemistry and the structure and dynamics of liquid-crystalline materials. Dr. Yannoni received his B.A. in chemistry from Harvard University in 1957 and his Ph.D. in physical chemistry from Columbia University in 1966. In 1978 he received an IBM Outstanding Contribution Award for his work on developing high-resolution NMR techniques for characterizing solids. In 1982, Dr. Yannoni served as chairman of the 23rd Experimental NMR Conference. He is a member of the American Chemical Society.